CHINESE OPTICS LETTERS

Vol. 23, No. 1 | January 2025

Linear optical characterization of meter-size zinc sulfide polycrystal

Xiaobo Zhao (赵小玻)[1], Kui Wu (武 奎)[1*], Dazhi Lu (路大治)[1**], Cong Zhang (张 琮)[2***], Haohai Yu (于浩海)[1], and Huaijin Zhang (张怀金)[1]

[1] State Key Laboratory of Crystal Materials and Institute of Crystal Materials, Shandong University, Jinan 250100, China

[2] Sinoma Synthetic Crystal (Shandong) Co., Ltd., Jinan 250000, China

*Corresponding author: wukui@sdu.edu.cn

**Corresponding author: dazhi.lu@sdu.edu.cn

***Corresponding author: zhangc_1984@163.com

Received June 12, 2024 | Accepted July 29, 2024 | Posted Online February 4, 2025

Zinc sulfide (ZnS) has promising linear and nonlinear optical properties and has shown important applications in military and modern devices. In this work, coupled with the chemical vapor deposition (CVD) method and hot isostatic pressing (HIP), we successfully grew a high-transmittance and low-absorption-coefficient polycrystalline ZnS with a size of 1 m × 2 m and a thickness of 20 mm. The linear optical properties, including the UV-vis-NIR transmission spectrum, infrared spectrum, and refractive index, were systematically characterized, which shows that the present ZnS polycrystal exhibits a wide transmission range from 0.34 to 15.00 μm, covering two important atmospheric windows. Moreover, its Sellmeier equation was achieved and fitted as a modification of previous studies. According to the refractive index and transmission spectrum, optical loss was calculated to be < 3.5% from 1 to 10 μm. All the results indicate that the present sample has comparable properties with the single crystals and should have potential applications as a functional material.

Keywords: ZnS; chemical vapor deposition; optical transmission; refractive index.
DOI: 10.3788/COL202523.011601

1. Introduction

Infrared (IR) optical materials have been widely used as window materials, aviation cowling, etc., which satisfy various applications in the military and civil fields[1–4]. Zinc sulfide (ZnS), which exhibits excellent optical and mechanical properties, has been developed as an important IR optical material with a large direct bandgap (3.6 eV) and a large exciton binding energy (39 meV)[5]. It is particularly valued for its high transmission range and refractive index, which are critical parameters for the manipulation and control of light in these fields. In the context of ZnS, its transmission properties are exceptional, especially in the visible and near-IR regions of the electromagnetic spectrum. ZnS exhibits high transparency, which is crucial for applications that require light to pass through with minimal absorption or scattering. Consequently, ZnS is often used in windows for IR applications, in lenses for optical systems, and as a host material for phosphors in lighting technologies. Up to now, several methods have been used to grow the ZnS material, such as hot-pressing (HP), physical vapor deposition (PVD), chemical vapor deposition (CVD), and CVD with hot isostatic pressing (HIP)[6–9]. However, it is still a challenge in the preparation of meter-size polycrystalline ZnS with high quality, which has important requirements in the development of high-power lasers, large-size lenses, windows, etc. By contrast, the CVD method has advantages in growing larger and more dense polycrystalline ZnS, and the HIP method could improve the sample quality. Therefore, it could be possible to grow high-quality and large-size polycrystalline ZnS by combining it with the CVD and HIP methods.

In this work, we have successfully grown standard polycrystalline ZnS by coupled CVD and HIP methods, and ZnS with a size of 1 m × 2 m and a thickness of 20 mm was obtained. The optical performance was investigated. Scanning electron microscopy (SEM) was used to observe the micro-structural changes, and no cracks or defects were observed, indicating its high growth quality. Other optical properties (UV-vis-NIR transmission spectrum and IR spectrum) were also measured, which shows that ZnS has a wide transmission range from 0.34 to 15.00 μm. The refractive index was measured with a wavelength of 400 to 2325 nm, and the Sellmeier equation was also determined.

2. Experiment

A polycrystalline tablet of ZnS was prepared by the CVD method, and its quality was further improved by HIP treatment [Figs. 1(a) and 1(b)]. The initial ingredients for the CVD furnace were zinc-ingot and H_2S air, which were loaded and heated to 500–750°C with a vacuum degree of 1000–3000 Pa. Within the chamber, H_2 and Ar gases were aerated as carrier gas together with Zn vapor. Graphite plates served as the deposition substrate, and the experiment ran from seven to thirty days. Excess Zn was used in the experiment with $n(\mathrm{Zn}):n(\mathrm{S})=1.2:1$. The following reaction happened in the growth process:

$$\mathrm{H_2S(V)} + \mathrm{Zn(V)} \rightarrow \mathrm{ZnS(S)} + \mathrm{H_2(V)}.$$

In ZnS CVD, it will undergo the following processes, including sublimation, chemical transport, and chemical synthesis. In order to create structurally complete ZnS crystals with outstanding optical qualities, stable growth can be sustained for a lengthy period of time when the physical, chemical, and thermodynamic parameters align with those necessary for crystal nucleation. Finally, high-transmittance ZnS with a size of 1 m × 2 m and a thickness of 20 mm was obtained [Figs. 1(a) and 1(b)].

The HIP method was performed as heat treatment of CVD ZnS to improve the optical properties. Typical temperatures and pressures used are 1010°C at 100–200 MPa with a duration of 120 h.

X-ray diffraction (XRD) and energy dispersive spectroscopy (EDS) were performed for component and stoichiometric ratio analysis (40 kV, Cu, 5 deg/min, step 0.02 deg).

The surface morphology and micro-structure of grown ZnS were observed by an S-4800 SEM. The UV-vis-NIR and IR transmission spectra were measured from 200 to 1300 nm and 400 to 4000 $\mathrm{cm^{-1}}$, respectively. The refractive index was measured with a wavelength of 400 to 2325 nm by SpectroMaster UV-VIS-IR (Trioptics, Germany) at room temperature.

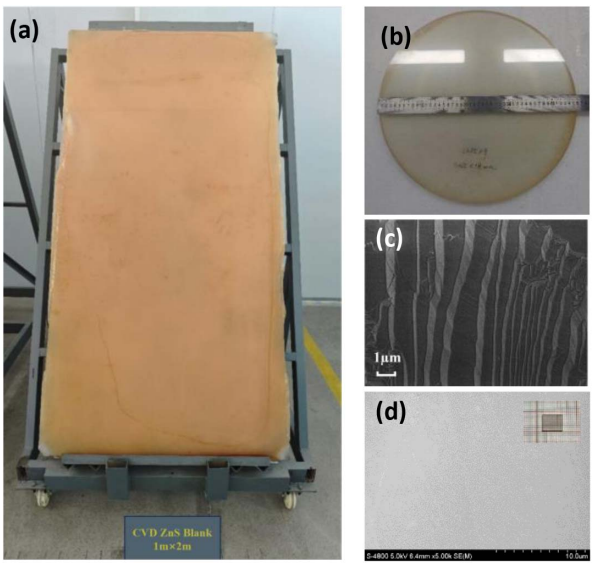

Fig. 1. (a) ZnS tablet with a size of 1 m × 2 m. (b) Polished transparent ZnS plate after HIP (Ø45 × 18 $\mathrm{mm^3}$). (c) Micro-structure from SEM and (d) surface morphology from SEM with the measured ZnS sample in the upper right corner (10 mm × 8 mm × 2 mm).

3. Results and Discussion

Micro-structure characterization in Fig. 1(c) shows that the grown ZnS materials have a uniform grain size of 1–10 μm. The sample from grown ZnS is shown in Fig. 1(d) in the upper right corner with dimensions of 10 mm × 8 mm and is used for the following test. From the surface morphology observed by SEM [Fig. 1(d)], it reveals that almost all of the porosity was removed after the HIP process, and no cracks or growth boundaries were observed, which indicates that grown ZnS polycrystalline possesses high quality and homogeneity. This result also verifies that high-quality ZnS can be used for IR applications without harmful optical diffraction.

For CVD growth, it is crucial to find an equilibrium point of temperature, pressure, and gas flow rates to obtain intact ZnS tablets. Temperature is a key factor that affects the reaction kinetics and the rate of deposition[10]. Higher temperatures can increase the reaction rate but may also lead to undesirable side reactions. It was discovered that the temperature at which the polycrystalline zinc sulfide was deposited greatly affected the size of the grain[11]. A higher temperature of deposition produced bigger grains. Standard CVD zinc sulfide was typically opaque (i.e., strongly scattering) to the eye and ranged in apparent hue from colorless to yellow to orange to red to brown to even black. Pressure plays a role in controlling the concentration and residence time of the precursor gases, which in turn affects the deposition rate and uniformity[12]. Gas flow rates determine the number of precursors available for reaction, and their optimization is essential for consistent film growth[13]. The uniformity of the deposition thickness is more influenced by reactant flow rates (metered rates of argon carriers for Zn vapor and H_2S) than by visible transmission in particular. Dibenedetto *et al.*[14] demonstrated that ZnS material with a greater sulfur content and worse optical quality (i.e., more scatter) was produced in regions with higher sulfur partial pressures, such as those close to H_2S intake jets. This implies that the vapor furthest from the H_2S injectors will be more zinc-rich and contain less sulfur, which can lead to superior optical quality. The material selection for the substrate is considered to be a way to catalyze the surface reaction for the initial material to be deposited. Alumina, fused silica, and molybdenum were examined for the first steps, but it was discovered that they were too reactive, which affected the deposited ZnS material or the substrates' capacity to be reused[15]. Graphite substrates are still widely used today since they were discovered to be the most resilient and nonreactive. In an investigation conducted[16], the usage of graphite versus tantalum substrates was compared to see if there was a difference in the optical characteristics, but none was discovered. Therefore, noncatalytic, unreactive

substrates are preferable, and the original substrate materials have little bearing on the ZnS material's quality.

HIP is recognized as an effective method to improve the quality of ZnS. Previously reported results show that the HIP process can enhance the optical quality of ZnS through eliminating the tiny pores after hot-pressing and this treatment is particularly beneficial for multi-spectrum transparent ceramics and preventing the phase change from cubic to hexagonal structure at the suitable high pressure[17,18]. Moreover, this HIP method can also eliminate the potential impurities such as oxygen and hydrogen. Therefore, optical transmission of ZnS after HIP can be enhanced to a level comparable to single crystals, which is also verified by the following test.

XRD and EDS were performed for component and stoichiometric ratio analysis, and the measured results are shown in Fig. 2. Figure 2(a) shows that the experimental XRD patterns of grown ZnS are consistent with the standard one. Figures 2(b) and 2(c) are the SEM photo and EDS of the measured sample, and the results show that the stoichiometric ratio of Zn:S is not typically 1:1 since excess Zn was used in the growth experiments.

The refractive index was served to assess the optical characteristic that is essential for designing optical equipment and determining internal optical paths. High optical quality ZnS was cut into prisms along the growth direction. Refractive index measurements were performed on SpectroMaster UV-VIS-IR at 11 specific wavelengths ranging from 0.400 to 2.325 μm, and the results are listed in Table 1. As seen in Fig. 3, its refractive index shows a decreasing trend with increasing wavelength.

The dispersion parameters for the Sellmeier equation were fitted by the least squares method. The fitted Sellmeier equation for the refractive index is shown in Table 2, where n is the principal refractive index and λ is the wavelength. Compared with

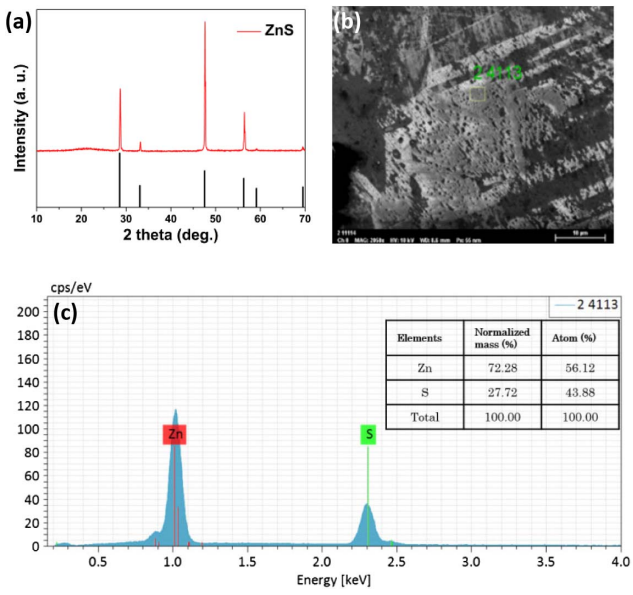

Fig. 2. (a) XRD patterns of the grown ZnS; (b) SEM image of the ZnS sample used for EDS analyses; (c) EDS analyses results for the sample shown in (b).

Table 1. Comparison of Measured and Fitted Refractive Indices.

λ (μm)	Measured refractive index	Fitted refractive index
0.4047	2.5281966	2.527736001
0.4358	2.4734018	2.474110722
0.4800	2.4221488	2.422468522
0.5461	2.3745115	2.374299764
0.5875	2.3544081	2.354088187
0.6438	2.3341786	2.33383809
0.7065	2.3178797	2.317632451
0.8521	2.2941409	2.294236568
1.0140	2.2794293	2.279861088
1.5300	2.2606278	2.260728303
2.3250	2.2505997	2.250516680

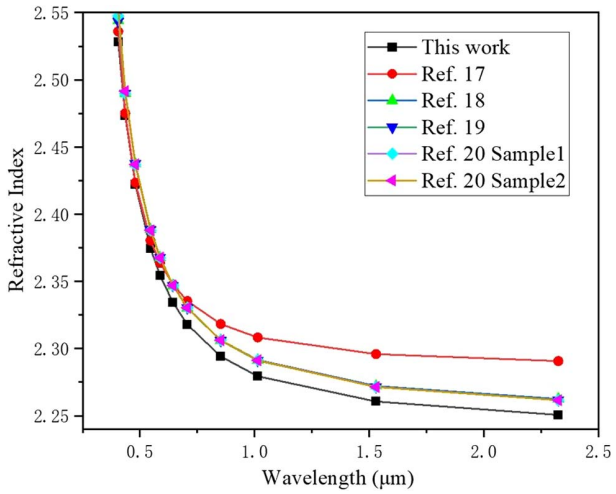

Fig. 3. Refractive index of ZnS polycrystalline along the growth direction.

previous different forms of the Sellmeier equation, also listed in Table 2 and shown in Fig. 2, we provided a modified Sellmeier-type dispersion and amendment to describe the available data of optics studies with the refractive index. According to the equation, we have also calculated the change rule between the refractive index and wavelength. As shown in Fig. 3 and Table 1, the calculated refractive indices based on the Sellmeier equation agree well with the experimental values to within acceptable experimental errors.

The UV-vis-NIR transmission spectrum of the polished ZnS sample with a thickness of 1 mm was determined with a wavelength of 200 to 1300 nm (Fig. 4). The measured result shows that ZnS has a high transmittance (>70%) within 400–1300 nm and its UV cut-off wavelength is located at 340 nm. Moreover, its

Table 2. Different Expressions of the ZnS Sellmeier Equation.

Ref.	Sellmeier equation of ZnS materials
[19]	$n^2_{(\lambda)} = 4.17 + \frac{1.06\lambda^2}{\lambda^2-0.087}$
[20]	$n^2_{(\lambda)} = 8.393 + \frac{0.14383}{\lambda^2-0.2421^2} + \frac{4430.99}{\lambda^2-36.71^2}$
[21]	$n^2_{(\lambda)} = 8.34096 + \frac{0.14540}{\lambda^2-0.23979^2} + \frac{3.23924}{\lambda^2/36.525^2-1}$
[22]	$n^2_{(\lambda)} = 1 + \sum_{i=1}^{3} \frac{A_i\lambda^2}{\lambda^2-\lambda_i^2}$

Parameters for different samples	
$A_1 = 0.33904026$	$A_1 = 0.24199447$
$A_2 = 3.7606868$	$A_2 = 3.8575584$
$A_3 = 2.7312353$	$A_3 = 2.5433609$
$\lambda_1 = 0.31423026$	$\lambda_1 = 0.33005445$
$\lambda_2 = 0.17594174$	$\lambda_2 = 0.17899635$
$\lambda_3 = 33.886560$	$\lambda_3 = 32.849275$

This work $n^2_{(\lambda)} = 5.05914 + \frac{0.137897}{\lambda^2-0.0601717} - 0.00372052 \times \lambda^2$

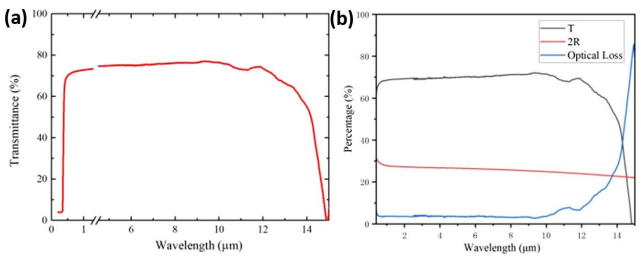

Fig. 4. (a) ZnS transmission spectrum from the ultraviolet to infrared region. (b) Optical loss from 0.4–15 μm.

bandgap is also calculated to be 3.65 eV[8], which is consistent with the previously reported values[23]. Moreover, the IR spectrum is also measured to determine the IR transmission region. With the polished ZnS polycrystalline slice, the IR spectrum was also tested within the range of 400 to 4000 cm^{-1}, and the result shows that ZnS has a high transmittance (>70%) from 2.5 to 12 μm and its IR cut-off edge is located at 15 μm. Thus, ZnS has a wide transmission range from 0.34 to 15.00 μm, which covers two important atmosphere windows (3–5 and 8–12 μm). The high transmission can be explained by the increment in the densification rate after the HIP process. It is worth noting that there is no obvious absorption at 9 and 10–11 μm, which may be caused by the vibration of SO_4^{2-}[24] and SO_3^{2-}[25] groups. Because these two groups easily result from the absorption of oxygen by exposure to the air on the surface of ZnS, therefore, no absorption at these wavelengths means good thermal stability with bond variation in grown ZnS materials.

Optical loss analyses were carried out in the wavelength range of 400–1500 nm shown in Fig. 3(b). According to $I_{sum} = I_{trans} + I_{abs} + I_{refl} = 1$, among which reflectance R% and refractive index n satisfy the following equation:

$$R = \frac{(n_1 - n_2)^2}{(n_1 + n_2)^2}.$$

From the refractive index data, the single specular reflectance was calculated, and due to the reversibility of the optical path, this resulted in two specular reflectances of $[R + (1 - R)^* R]$%. From the results, the absorption in the grown ZnS materials is below 3.5% from 1 to 10 μm, indicating excellent optical qualities with an absorption coefficient of 3.3 cm^{-1}. With the wavelength longer than 10 μm, the ZnS absorption increases with a wavelength due to the intrinsic absorption.

Herein, we have also compared the optical properties of ZnS with other known IR materials (such as Si, Ge, Ti Al_2O_3, MgF_2, and CaF_2), and the data are shown in Table 3. Grown polycrystalline ZnS has the widest transmission range and relatively high transmittance (0.34–12 μm, $T > 70\%$) that was determined by its wide bandgap, which prevents the absorption of light within these wavelength ranges. These results indicate that large-size polycrystalline ZnS grown by the CVD method can be viewed as an excellent IR window material because of its high optical quality and IR transmission range.

Table 3. Transmittance and Refractive Indices of Common Infrared Materials.

	Refractive index at 530 nm	Transmittance	IR cut-off edge (μm)
ZnS (this work)	2.3677	75% at 0.4–12 μm	14
Silicon[26]	3.422	55% at 1.5–6.5 μm	10
Germanium[27]	4.003	50% at 2–10 μm	12
Sapphire[28]	1.768	88% at 0.16–4 μm	5
Magnesium fluoride[29]	1.413	91% at 3–7.5 μm	10
Calcium fluoride[30]	1.434	87% at 3–5 μm	10

4. Conclusion

In this work, the growth of meter-size polycrystalline ZnS by the CVD method was reported. The SEM test shows that polycrystalline ZnS has high optical quality and that no cracks are found in the ZnS surface. Surface morphology post-HIP treatment revealed a significant reduction in porosity and the absence of cracks, signifying a homogeneous and high-quality material suitable for optical application. Property measurement shows that ZnS has a wide IR transmission region (0.34 to 15.00 μm) and high transmittance (0.4–12.0 μm, >70%). Its Sellmeier equation is also deduced from the measured refractive index, and it shows a good consistency between calculated and experimental values, which offers a modification of previous research about the refractive index of ZnS. The optical loss was calculated below 3.5% in the range of 1–10 μm, which means high qualities of grown ZnS. This research result indicates that the CVD method is an effective method to grow large-size, high-quality polycrystalline ZnS, and grown polycrystalline ZnS has excellent properties to be used as IR window materials.

Acknowledgements

This work was supported by the National Natural Science Foundation of China (Nos. 52025021, 52372009, and 52272004) and the Qilu Young Scholar Program of Shandong University.

References

1. H. Nie, F. Wang, J. Liu, *et al.*, "Rare-earth ions-doped mid-infrared (2.7–3 μm) bulk lasers: a review [Invited]," Chin. Opt. Lett. **19**, 091407 (2021).
2. J. Zhao, S. Wang, C. Zhang, *et al.*, "Research status and challenges in the manufacturing of IR conformal optics," Def. Technol. **10**, 154 (2024).
3. D. C. Harris, "Frontiers in infrared window and dome materials," Proc. SPIE **2552**, 325 (1995).
4. J. Liu, L. Tang, X. Feng, *et al.*, "Mid-infrared SESAM mode-locked Er:CaF_2-SrF_2 bulk laser at 2.73 μm," Chin. Opt. Lett. **22**, 051406 (2024).
5. P. D'Amico, A. Calzolari, A. Ruini, *et al.*, "New energy with ZnS: novel applications for a standard transparent compound," Sci. Rep. **7**, 16805 (2017).
6. C. Li, T. Xie, J. Dai, *et al.*, "Hot-pressing of zinc sulfide infrared transparent ceramics from nanopowders synthesized by the solvothermal method," Ceram. Int. **44**, 747 (2018).
7. S. Yano, R. Schroeder, B. Ullrich, *et al.*, "Absorption and photocurrent properties of thin ZnS films formed by pulsed-laser deposition on quartz," Thin Solid Films **423**, 273 (2003).
8. X. Zhao, C. Zhang, Z. Wang, *et al.*, "Macro- and micro-structural manifestation and engineering of large-size polycrystalline ZnSe," CrystEngComm **26**, 1986 (2024).
9. D. Li, N. Wei, J. Yang, *et al.*, "Effects of hot isostatic pressing on the performance of CVD ZnSe," Opt. Mater. **132**, 112868 (2022).
10. A. Becker and K. J. Hüttinger, "Chemistry and kinetics of chemical vapor deposition of pyrocarbon — IV pyrocarbon deposition from methane in the low temperature regime," Carbon **36**, 213 (1998).
11. J. A. Savage, K. L. Lewis, A. M. Pitt, *et al.*, "The role of a CVD research reactor in studies of the growth and physical properties of ZnS infrared optical material," Proc. SPIE **505**, 47 (1984).
12. E. Vetrivendan, R. Hareesh, N. G. Krishna, *et al.*, "Effect of chemical vapor deposition pressure on preferred orientation, microstructure, and oxidation resistance of pyrolytic graphite," J. Mater. Eng. Perform. (2024).
13. J.-O. Carlsson and P. M. Martin, "Chemical vapor deposition," in *Handbook of Deposition Technologies for Films and Coatings* (2010), p. 314.
14. B. A. Dibenedetto and J. Pappis, "Chemical vapor deposition of multispectral domes," Final Report (Raytheon Co., 1975).
15. S. R. Steele and J. Pappis, "Chemical vapor deposition of IR materials," Technical Report AFAL-TR-71-200F33615-70-C-1577 (1971).
16. Y. Drezner, S. Berger, and M. Hefetz, "A correlation between microstructure, composition and optical transparency of CVD-ZnS," Mater. Sci. Eng. **87**, 59 (2001).
17. D. Li, N. Wei, J. Yang, *et al.*, "Effects of hot isostatic pressing on the performance of CVD ZnSe," Opt. Mater. **132**, 112868 (2022).
18. H. V. Atkinson and S. Davies, "Fundamental aspects of hot isostatic pressing: an overview," Metall. Mate. Trans. A **31**, 2981 (2000).
19. S. O. S. Ozaki and S. A. Sadao Adachi, "Optical constants of cubic ZnS," Jpn. J. Appl. Phys. **32**, 5008 (1993).
20. M. Debenham, "Refractive indices of zinc sulfide in the 0405–13-μm wavelength range," Appl. Opt. **23**, 2238 (1984).
21. H. H. Li, "Refractive index of ZnS, ZnSe, and ZnTe and its wavelength and temperature derivatives," J. Phys. Chem. Ref. Data **13**, 103 (1984).
22. A. Feldman, D. Horowitz, R. M. Waxler, *et al.*, Optical materials characterization, Semiannual Technical Report (National Bureau of Standards, 1976).
23. J. McCloy and R. Korenstein, "Variability in chemical vapor deposited zinc sulfide: assessment of legacy and international CVD ZnS materials," Proc. SPIE **7302**, 73020M (2009).
24. E. Khawaja and S. G. Tomlin, "The optical constants of thin evaporated films of cadmium and zinc sulphides," J. Phys. D Appl. Phys. **8**, 581 (1975).
25. O. L. Arenas, M. T. S. Nair, and P. K. Nair, "Chemical bath deposition of ZnS thin films and modification by air annealing," Semicond. Sci. and Technol. **12**, 1323 (1997).
26. S. G. Kaplan and L. M. Hanssen, "Silicon as a standard material for infrared reflectance and transmittance from 2 to 5 μm," Infrared Phys. Technol. **43**, 389 (2002).
27. H. Liu, S. Li, P. Sun, *et al.*, "Study on characterization method of optical constants of germanium thin films from absorption to transparent region," Mater. Sci. Semicond. Process. **83**, 58 (2018).
28. M. Tang, W. Zhu, H. Zou, *et al.*, "High strength and high light transmittance sapphire/sapphire joints bonded using a La_2O_3-Al_2O_3-SiO_2 glass filler," J. Eur. Ceram. Soc. **42**, 4607 (2022).
29. M. Tavakoli, B. Movahedi, and A. Alhaji, "Fluorination synthesis of MgF_2 nanoparticles synthesized for manufacturing IR windows by hot-pressing," Ceram. Int. **47**, 21285 (2021).
30. D. Hahn, "Calcium fluoride and barium fluoride crystals in optics," Optik Photonik **9**, 45 (2014).